Flow efficiency in multi-louvered fins

X. Zhang [a], D.K. Tafti [b],*

[a] *STM Power Inc., 275 Metty Drive, Ann Arbor, MI 48103, USA*
[b] *Department of Mechanical Engineering, Virginia Tech, 105 Randolph Hall, Blacksburg, VA 24061, USA*

Received 23 July 2002; received in revised form 16 November 2002

Abstract

The paper studies the effect of Reynolds number, fin pitch, louver thickness, and louver angle on flow efficiency in multi-louvered fins. Results show that flow efficiency is strongly dependent on geometrical parameters, especially at low Reynolds numbers. Flow efficiency increases with Reynolds number and louver angle, while decreasing with fin pitch and thickness ratio. A characteristic flow efficiency length scale ratio is identified based on geometrical and first-order hydrodynamic effects, which together with numerical results is used to develop a general correlation for flow efficiency. Comparisons show that the correlation represents more than 95% of numerical predictions within a 10% error band, and 80% of predictions within a 5% error band over a wide range of geometrical and hydrodynamic conditions.
© 2003 Elsevier Science Ltd. All rights reserved.

1. Introduction

Compact heat exchangers are used in a variety of automotive, residential air-conditioning and refrigeration applications. For air-side heat transfer augmentation, multi-louvered fins are quite popular. Beauvais [1] was the first to conduct flow visualization experiments on the louvered fin array. He demonstrated that louvers, rather than acting as surface roughness that enhanced heat transfer performance, acted to realign the airflow in the direction parallel to themselves. Davenport [2] performed flow visualization experiments identical to those of Beauvais and further demonstrated two flow regimes, duct directed flow, and louver directed flow. In general, the flow direction follows the path of least hydraulic resistance. Under certain conditions, one of them being low Reynolds number, the flow has a propensity to move straight through between fins, rather than align itself to the louvers. At low Reynolds numbers, this is a result of the high flow resistance between louvers brought about by the thick boundary layers.

The flow direction has profound implications on the overall heat capacity of the fin by virtue of its strong effect on the heat transfer coefficient. It is particularly crucial for low Reynolds number applications ($Re < 500$), in which the natural tendency for air is to flow straight through the fin and not over the louvers. Hence, it is important to be able to quantify and predict the flow direction.

Flow efficiency (η) is used to describe the percentage of the fluid flowing along the louver direction. A 100% efficiency represents ideal louver directed flow while 0% represents complete duct directed flow. In the past, two kinds of definitions of flow efficiency have been used. In experimental dye injection studies [3–6] flow efficiency is defined as the ratio of actual transverse distance (N) traveled by the dye to the ideal distance (D) if the flow were aligned with the louver.

$$\eta_{\exp} = \frac{N}{D}.$$

In numerical simulations, because the flow angle can be easily obtained for each individual louver, flow efficiency is defined to be the ratio of mean flow angle (α_{mean}), which is obtained by averaging flow angles throughout the louver bank (inlet, redirection and exit louvers are not included), to louver angle (θ) as follows:

* Corresponding author. Tel.: +1-540-231-9975; fax: +1-540-231-9100.

E-mail address: dtafti@vt.edu (D.K. Tafti).

Nomenclature

b	non-dimensional fin thickness (b^*/L_p^*)
d	characteristic flow efficiency length scale ratio
D_h	non-dimensional hydraulic diameter
f	friction factor
F_p	non-dimensional fin pitch (F_p^*/L_p^*)
F_d	non-dimensional flow depth
k	thermal conductivity
L_p^*	dimensional louver pitch (characteristic length scale), $L_p = 1$
Nu	non-dimensional heat transfer coefficient, $Nu = h^*L_p^*/k = (-\partial T/\partial n)/(1 - T_{ref})$
Re	Reynolds number, $Re_{in} = u_{in}^*L_p^*/v$, $Re_{L_p} = V_c^*L_p^*/v$
T_{ref}	mixed mean temperature
u	streamwise velocity (in x-direction)
v	cross-stream velocity (in y-direction)
u_{in}^*	dimensional inlet velocity (characteristic velocity scale)

V_c	average velocity at minimum cross-sectional area
x	streamwise direction
y	cross-stream direction

Greek symbols

η	flow efficiency, $\eta = \alpha_{mean}/\theta$
θ	degrees, louver angle
α	degrees, flow angle, $\alpha = \tan^{-1}((\int v\,dx/L_p)/(\int u\,dy/F_p))$
v	kinematic viscosity

Superscript

*	dimensional quantities

Subscripts

F	based on fin
L	based on louver
c	critical

$$\eta = \frac{\alpha_{mean}}{\theta}.$$

In the present paper, the average velocity ratio (the average normal velocity across top boundary to that across the left boundary) is used to define flow angle in an individual block surrounding a louver, as follows: [1]

$$\alpha = \tan^{-1}\frac{\int v\,dx/L_p}{\int u\,dy/F_p}.$$

For a small louver angle ($\theta < 30$), the difference between η_{exp} and η is small. [2]

Webb and Trauger (hereafter referred to as WT) [3] experimentally studied the flow structure in multi-louvered fin geometries for six fin pitch ratios (0.7–1.5), one thickness ratio (0.0423) and two louver angles (20° and 30°). Reynolds number (based on louver pitch) ranged from 400 to 4000. Their results showed that flow effi-

ciency increased with increasing Reynolds number until a critical Reynolds number was reached,

$$Re_{w,c} = 828\left(\frac{\theta}{90}\right)^{-0.34}. \tag{1}$$

Before the critical value, flow efficiency depends on, and increases with Reynolds number, louver angle, and decreases with fin pitch ratio.

$$\eta_w = 0.091Re^{0.39}\left(\frac{L_p}{F_p}\right)^{0.44}\left(\frac{\theta}{90}\right)^{0.3}. \tag{2}$$

Beyond the critical value, flow efficiency is only affected by fin pitch ratio.

$$\eta_{w,max} = 0.95\left(\frac{L_p}{F_p}\right)^{0.23}. \tag{3}$$

The above flow efficiency is not continuous at the critical Reynolds number. To remedy this deficiency, Eq. (2) was modified by Sahnoun and Webb (hereafter referred to as SW) [4] to keep the flow efficiency continuous at the critical Reynolds number:

$$\eta_w = 0.95\left(\frac{L_p}{F_p}\right)^{0.23} - 0.00003717$$
$$\times \left[828\left(\frac{2\theta}{\pi}\right)^{-0.34} - Re\right]^{1.1}\left(\frac{L_p}{F_p}\right)^{-1.35}\left(\frac{2\theta}{\pi}\right)^{-0.61}.$$

It is interested to note that in SW's correlation, the critical Reynolds number depends only on louver angle

---

[1] The flow angle (α) has also been defined as the ratio of mass flow rates:

$$\alpha_A = \tan^{-1}\left(\int_0^{L_p} v\,dx \Big/ \int_0^{F_p} u\,dy\right).$$

This definition is inconsistent for $F_p \neq 1$. For example when the flow is louver directed $v = u\tan(\theta)$,

$$\alpha_A = \tan^{-1}\left[\frac{L_p}{F_p}\tan(\theta)\right] \neq \theta.$$

[2] $\eta_{exp} = \frac{N}{D} = \frac{\tan(\alpha_{mean})}{\tan(\theta)} \approx \frac{\alpha_{mean}}{\theta} = \eta.$

while the flow efficiency beyond this Reynolds number depends only on fin pitch ratio.

Achaichia and Cowell (hereafter referred to as AC) [7] used numerical calculations to model the flow through a simplified two-dimensional louver array. The louvers were assumed to be infinitely thin, and the flow to be fully developed. The fully developed assumption and zero thickness will overpredict the flow efficiency, particularly as the louver angle decreases and the fin pitch increases. In these geometries, there is a "development length" for flow efficiency before it achieves its "fully-developed" value. AC's simulations do not resolve this. From their numerical simulations, the following correlation for flow efficiency was given:

$$\eta_A = \left(0.936 - 243/Re - 1.76(F_p/L_p) + 0.995\theta\right)/\theta. \quad (4)$$

As Reynolds number tends to infinity, flow efficiency in equation (4) approaches an asymptotic value depending on fin pitch ratio and louver angle:

$$\eta_{A,max} = \left(0.936 - 1.76(F_p/L_p) + 0.995\theta\right)/\theta.$$

The critical Reynolds number for $\eta_A/\eta_{A,max} = 0.95$ is:

$$Re_{A,c} = \frac{4860}{(0.936 - 1.76(F_p/L_p) + 0.995\theta)}.$$

In 1996, Bellows (hereafter referred to as B) [5] conducted flow visualization experiments and investigated the effect of fin pitch ratio and louver angle on flow efficiency. Using AC's correlation as a starting point, and taking into consideration developing flow effects, a general correlation was developed as:

$$\eta_B = \left(-5 - 300/Re - 10(F_p/L_p) + 1.34\theta\right)/\theta. \quad (5)$$

The asymptotic flow efficiency as Reynolds number tends to infinity is:

$$\eta_{B,max} = \left(-5 - 10(F_p/L_p) + 1.34\theta\right)/\theta$$

and the critical Reynolds number for $\eta_B/\eta_{B,max} = 0.95$ is:

$$Re_{B,c} = \frac{6000}{(-5 - 10(F_p/L_p) + 1.34\theta)}.$$

To summarize, flow efficiency is a function of Reynolds number and geometrical parameters, fin pitch ratio and louver angle at low and intermediate Reynolds number. Flow efficiency increases with increase of Reynolds number and louver angle, and decreases with fin pitch ratio. As Reynolds number increases, flow undergoes a transition from duct directed flow (low efficiency) to louver directed flow (high efficiency). There exists a critical Reynolds number beyond which the flow efficiency is independent of Reynolds number. All previous correlations agree in predicting the general trends. However, substantial quantitative differences exist.

Fig. 1(a) plots the critical Reynolds numbers from previous correlations. SW's values are much higher than that of AC's and B, especially at large louver angle. On the other hand, the difference between B and AC is small. Fin pitch ratio has a small effect on critical Reynolds number at large louver angle. Fig. 1(b) plots the asymptotic flow efficiency from these correlations. B's results show the strongest dependence on both fin pitch ratio and louver angle, whereas the least is shown in SW's results. As fin pitch increases to 1.5, the flow efficiency in SW's results can be more than two times larger than that in B's at $\theta = 20$. In Fig. 1(c), contrary to other results, flow efficiency in WT's experiments shows a near linear increase in flow efficiency with the Reynolds number (concave curve with log scale), during the transition from duct to louver directed flow. Fig. 1(c) also shows that, before modification, WT's results show better agreement with others at very low Reynolds number, whereas results of SW and WT agree better beyond Reynolds number 50.

An important omission in all previous correlations (both numerical and experimental) is the effect of fin thickness ratio. The fin thickness ratios are completely different in these studies. Thickness ratio in AC's numerical calculations is zero, in B's experiments, it varied from 0.089 to 0.106, while in WT's experiments it was fixed at 0.0423.

Our objective in this paper is to use over 200 high resolution numerical simulations done over the past three to four years to develop a broader and consistent relationship between flow efficiency and multi-louver geometry and Reynolds number. We study the effect of fin pitch, louver angle, fin thickness, and flow depth on flow efficiency to obtain a mathematical model, which is then used to develop a correlation for flow efficiency.

2. Numerical method and computational geometry

The governing equations for momentum and energy conservation are solved in a general boundary conforming coordinate system. They are discretized with a conservative finite-volume formulation. Details about the time-integration algorithm, treatment of boundary and louver surface conditions, and validation of the computer program can be found in Tafti et al. [8]. The base configuration used in these calculations consists of an entrance and exit louver with four louvers on either side of the center or redirection louver. Fig. 2 shows the base fin geometry and the corresponding computational domain which is resolved by 15 computational blocks, one for each louver, two each for the entrance, exit and redirection louver. The exit domain extends approximately 5.5 non-dimensional units downstream of the exit louver. Periodic boundary conditions are applied in
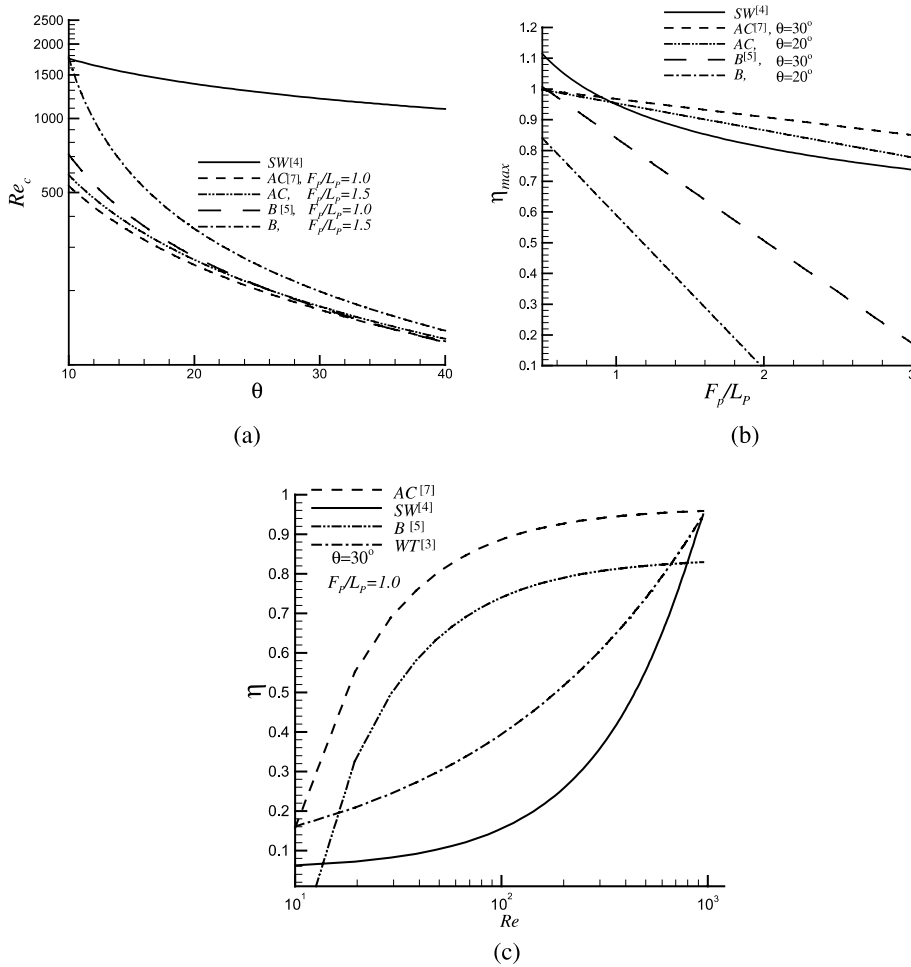
Fig. 1. Previous correlation results. (a) Critical Reynolds number versus louver angle; (b) asymptotic value of flow efficiency versus fin pitch ratio; (c) flow efficiency versus Reynolds number. Note the large qualitative as well as quantitative discrepancies between the correlations.
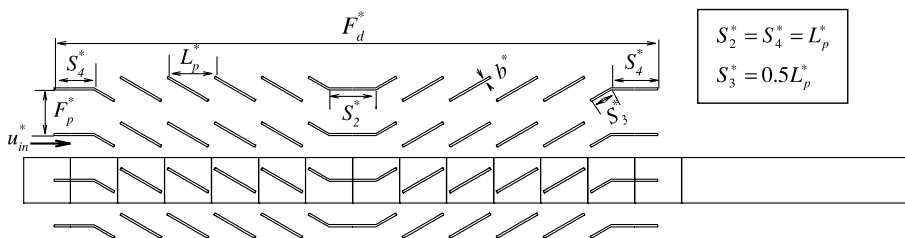

Fig. 2. Geometrical parameters of louvered fins and multi-block computational domain. The domain is resolved into 15 blocks, one for each louver, two each for the entrance, exit and middle louver. An exit domain (containing no louver), which extends approximately 5.0 non-dimensional units downstream of the array, is added to ensure that the fully developed boundary condition can be applied at the exit.

the transverse direction, while Dirichlet boundary conditions are specified at the entrance to the array.

All results reported in this paper are for a resolution of 96×96 cells per block (total resolution of 138,240

Table 1
Summary of non-dimensional geometrical parameters for the basic cases investigated

F_p	θ	b	F_d
1.0	30	0.05	13
		0.1	
		0.15	
	25	0.1	
	20	0.05	
		0.1	
		0.15	
	15	0.1	
1.5	30	0.1	17
	25		13
	20		13
	15		

Nominal Reynolds number range varied from $Re_{in} = 50$ to 1200.

cells). For the unsteady cases, time-averaged values are presented. The average momentum, energy, and mass residues are of the order of 1×10^{-8} at each time step.

Table 1 summarizes the base geometrical parameters studied in this paper. Two fin pitch ratios (1.0 and 1.5) are studied with variations in louver angle (15°, 20°, 25°, and 30°), and three thickness ratios (0.05, 0.1 and 0.15) are chosen. Reynolds number based on louver pitch is nominally varied from 50 to 1200.

3. Validation and evaluation of the current numerical method

A grid independency study was performed at a resolution of 128×128 cells in each block (a total of 245,760 cells). As shown in Fig. 3, the time averaged mean flow angles at most of the louvers are identical. Both, non-dimensional heat capacity and Nusselt number calculated on the 96×96 grid are within one percent of the fine grid calculation (not shown).

To further validate the numerical procedure, we have simulated the multi-louvered geometry used in the experiments of Dejong and Jacobi [6]. They performed flow visualization experiments to obtain flow efficiencies together with mass transfer experiments to quantity the heat transfer coefficient. In the experimental setup, the ratio of fin pitch to louver pitch is 1.09, thickness ratio is 0.1, and louver angle is set to 28°, with seven louvers on either side of the redirection louver. Results from the numerical simulations on an identical geometry are shown in Fig. 4(a)–(d). Fig. 4(a) and (b) compares the experimental dye path with streamlines injected at the inlet plane of the louver bank (flow is from right to left) at a Reynolds number of 400. The dye, injected between
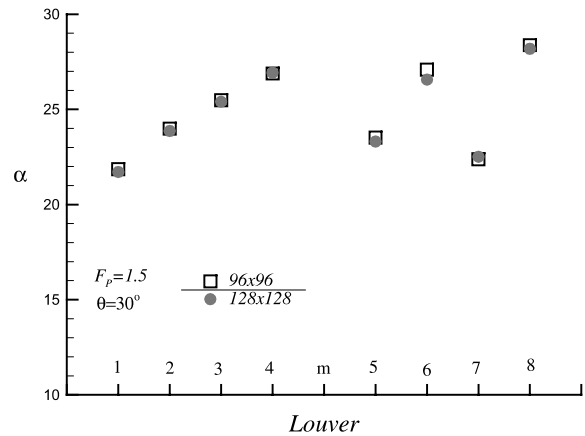

Fig. 3. A comparison of louver by louver distribution of flow angles at Reynolds number of 1000 for two mesh resolutions per computational block.

the first and second rows, traverses to the fifth row at the redirection louver. The experimental flow efficiency is: [3]

$$\eta_{exp} = \frac{N}{D} = \frac{3.5 F_p}{9 L_p \tan(28°)} = 0.797.$$

The streamline pattern obtained from the numerical simulations is nearly identical to the experiments. The average flow angle for the upstream louvers is 22.76°, whereas it is 22.98° for the downstream louvers. The calculated flow efficiency is: $\eta = \alpha_{mean}/\theta = 22.87°/28° = 0.81$, which agrees very well with the experiments (within 2%).

Fig. 4(c) compares the numerical versus experimental flow efficiencies for three Reynolds numbers. In general, the numerical flow efficiencies are predicted slightly higher than the experiments. Fig. 4(d) plots the experimental and numerical Nusselt numbers. The Sherwood number in DeJong's report for the whole louvered fin is 23.5 [4] at the Reynolds number 400, which corresponds to a Nusselt number of 15.76. This compares well with the numerical value of 15.77. Similar good agreement is obtained at Reynolds numbers = 150, 700 and 990.

4. Results

4.1. Effect of fin pitch ratio and louver angle

Fig. 5(a) plots flow efficiency versus Reynolds number for different fin pitch ratios and louver angles for

---

[3] In DeJong and Jacobi's report, it was 0.77.

[4] The Sherwood number in Dejong's experiments for this geometry is only available at $Re = 270$ and 600.
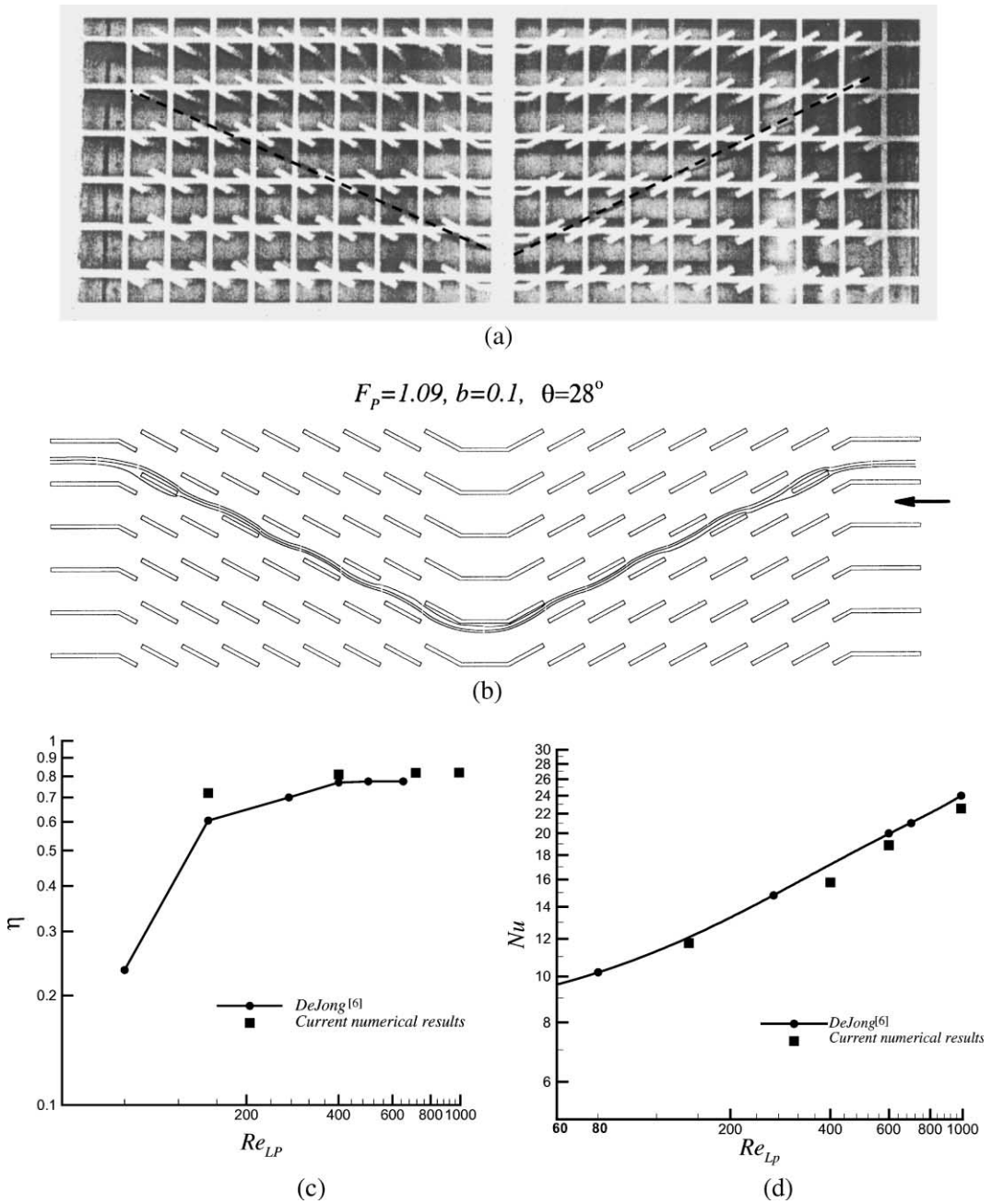
$$F_P = 1.09, \quad b = 0.1, \quad \theta = 28°$$

Fig. 4. (a) and (b) Comparison between calculated streamlines from numerical simulations and dye flow trace from experimental tests. Flow is from right side and is nearly parallel to louver direction at the Reynolds number 400; (c) comparison of flow efficiency; (d) the comparison of the Nusselt number.

developing flow in the louver bank. Results show a strong dependency on both these parameters. Generally, flow efficiency increases with increase in Reynolds number and louver angle, and with decrease in fin pitch ratio. At $Re_{in} = 50$, flow efficiency increases by 33% after

reducing the fin pitch ratio from 1.5 to 1.0 for 30° louvered fins, whereas a more than 130% increment is found when louver angle is increased from 15° to 30° for the same fin pitch ratio of 1.0. It is found that the asymptotic value of flow efficiency depends on fin pitch ratio as
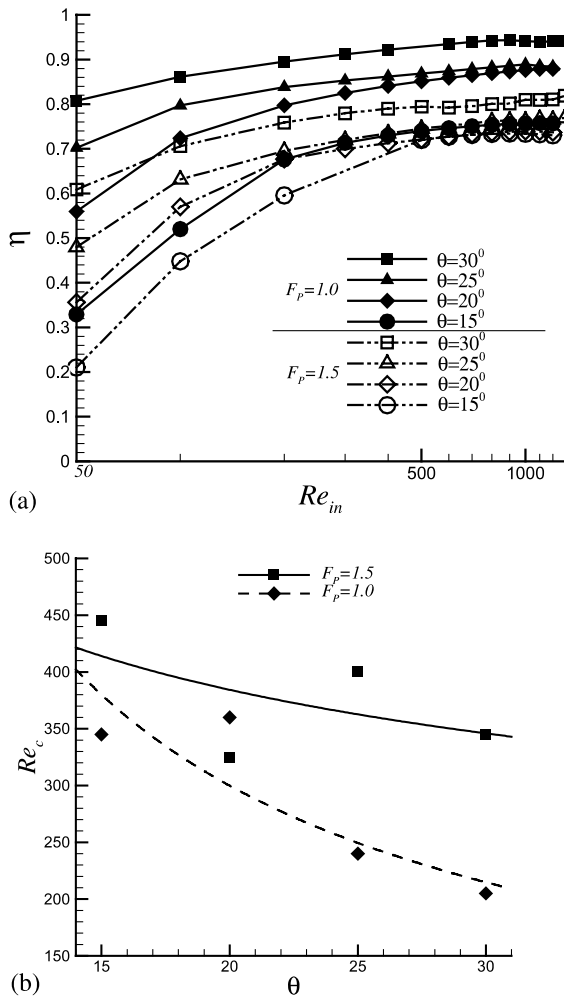
(a)

(b)

Fig. 5. (a) Flow efficiency versus Reynolds number with different fin pitch ratios and louver angles; (b) critical Reynolds number (at which the flow efficiency reaches 95% of the asymptotic value) versus louver angle for two fin pitch ratios.

well as louver angle. For the small fin pitch ratio, $F_p = 1.0$, the asymptotic value varies from 0.75 for 15° louvers to 0.94 for 30° louvers, whereas smaller variations are present for the larger fin pitch ratio studied. It is observed that the effect of louver angle is stronger for smaller fin pitch ratio. The rate of increment of flow efficiency in the transition region from duct to louver directed flow decreases rapidly with increase of Reynolds number, which is consistent with the results of AC and B, and contrary to the results of SW where nearly a constant rate of increase was found.

Fig. 5(b) plots the critical Reynolds number versus louver angle. Critical Reynolds number is based on the Reynolds number at which the flow efficiency reaches 95% of the maximum flow efficiency. The critical Rey-

nolds number decreases with increase in louver angle, and decrease in fin pitch. Hence at low Reynolds number, small fin pitch ratio and large louver angles are favorable for high flow efficiency. This trend is consistent with previous correlations of AC and B. For a fin pitch ratio of 1.0° and 15° louvered fins, the critical Reynolds number in the current study is around 350, which agrees well with 360 in AC and B's results, whereas in SW's results the critical Reynolds number is almost as high as 1500.

4.2. Effect of thickness ratio and flow depth

In previous experimental and numerical work, the effect of fin thickness on flow efficiency has not been studied, nor has it been included in correlations of flow efficiency. Fig. 6(a) plots the flow efficiencies with three different thickness ratios (0.05, 0.1, 0.15) at two louver angles, 20° and 30°. The results show the clear dependency on thickness ratio: thicker louvers lower flow efficiency for both louver angles; the deterioration of flow efficiency with thickness is more severe at small louver angles. At low Reynolds number ($Re_{in} = 50$), more than a 55% increment is found on reducing the thickness from 0.15 to 0.05 in 20° louvered fins, whereas only a 13% increment is found in the 30° geometry.

It is observed that for thicker fins ($b = 0.15$), a drop in flow efficiency is incurred as the Reynolds number increases beyond a certain value, followed by a recovery. At small louver angles the drop in flow efficiency occurs earlier than with large louver angles. As louver thickness increases, the open flow area between adjacent louvers is reduced. The percentage reduction in the flow area is larger for smaller louver angles. As Reynolds number increases, thicker louvers are more prone to develop large recirculation zones on the louver surface. The recirculation zones further block the flow path between louvers, hence decreasing the flow efficiency. As the Reynolds number increases further, the separated shear layer becomes unstable, with subsequent vortex shedding. This partially frees up the flow passage between louvers, and lets the flow efficiency recover to a higher value. This is seen in the distribution of flow angles at individual louvers in Fig. 6(b). The flow angles are higher at $Re_{in} = 500$, than at 1000 when recirculation zones dominate the flow field around louvers.

The effect of flow depth on flow efficiency was investigated by performing additional numerical calculations for the louvered fins with two more louvers on either side of the redirection louver for a 1.5 fin pitch ratio, 30° louver angle and 0.1 thickness ratio. The increase in flow depth has very little effect on flow efficiency, as shown in Fig. 6(c). For Reynolds number less than 300, two more calculations were also made for louvered fins with a 1.41 fin pitch ratio, 20° louver angle, and 0.15 fin thickness ratio. One configuration had 12
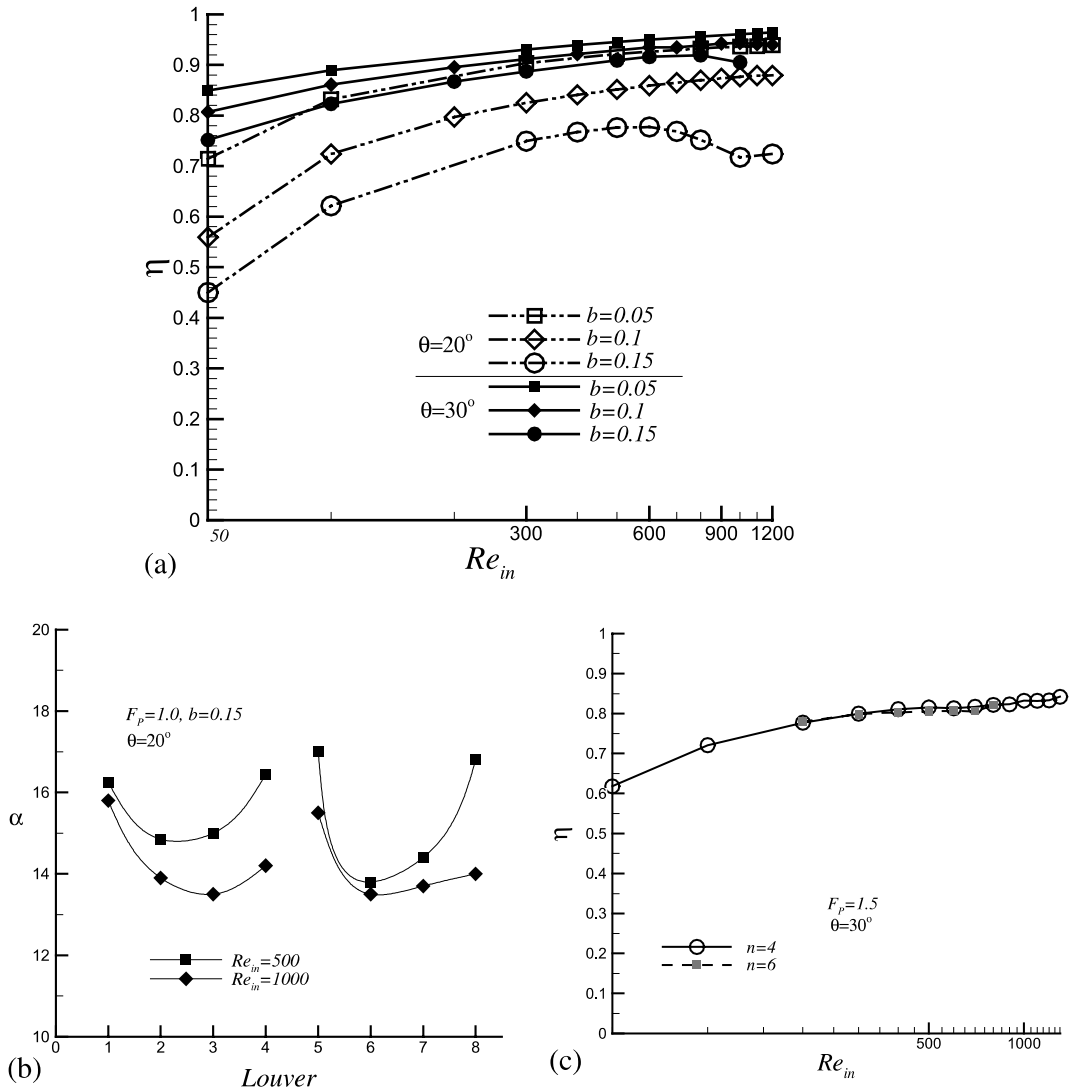
Fig. 6. (a) Flow efficiency versus Reynolds number for different thickness ratios and louver angles; (b) flow angles at two Reynolds numbers, 500 and 1000; (c) effect of flow depth on flow efficiency (n denotes number of louvers on either side of redirection louver).

louvers (six louvers on either side of redirection louver) and the other 14. At Reynolds number 50, flow efficiency for the two was identical.

4.3. Model for predicting trends in flow efficiency

The accurate prediction of flow efficiency requires that all geometrical and nonlinear hydrodynamic effects be taken into account. In this section we develop a simple model for predicting flow efficiency based solely on geometrical information and its first-order effect on the hydrodynamics. Using this model and the database of calculated flow efficiencies, we then develop a general correlation for flow efficiency in the next section.

For a given fin geometry and Reynolds number, air flow through the louver bank follows the path of least resistance. The incoming flow can be decomposed into two fluid streams: one that flows between two fins or duct directed flow, and the other which flows in the louver direction as shown in Fig. 7(a). If U_F is the bulk flow velocity in the direction parallel to the fin, and U_L, the bulk velocity parallel to the louver direction, then using the decomposition in Fig. 7(b), the following relationship is satisfied:

$$\tan \alpha = \left(\frac{U_L \sin \theta}{U_F + U_L \cos \theta} \right). \tag{6}$$
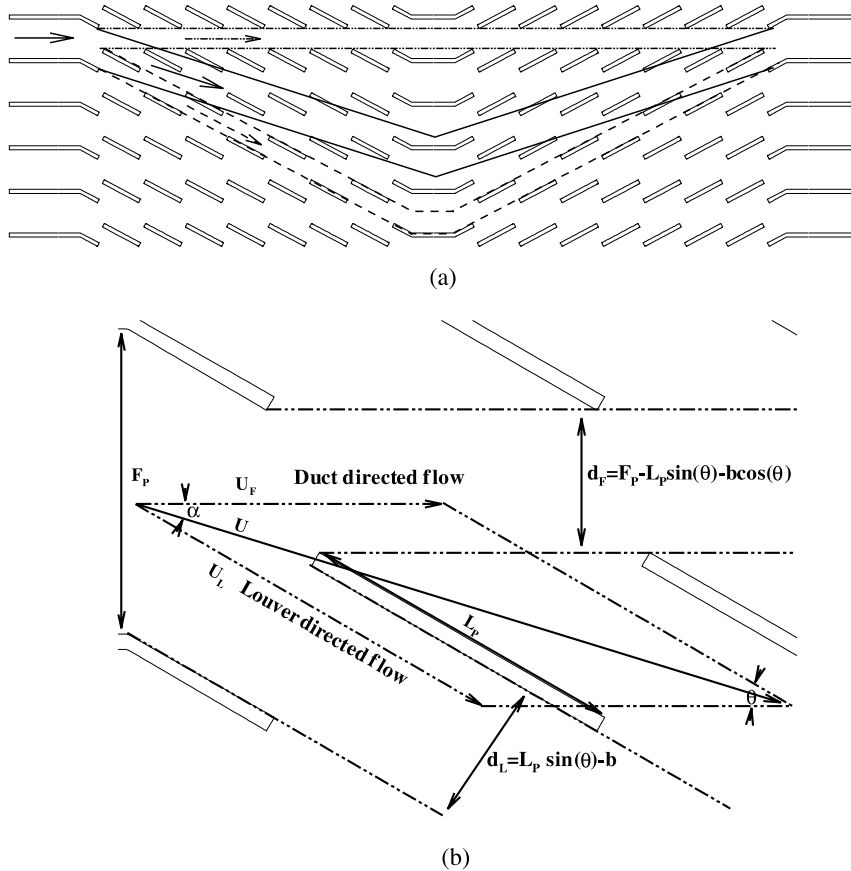
(a)

(b)

Fig. 7. Schematic plot of flow in multi-louvered fins. The channel bounded with solid lines represents the actual flow path, the channel with dash lines represents ideal louver directed flow, whereas dash-dot channel represents duct directed flow. In the analytical model, the actual flow passage is decomposed into the two ideal flow passages: duct directed and louver directed channels.

In the small to medium angle limit, Eq. (6) can be simplified to obtain an expression for flow efficiency as:

$$\eta = \frac{\alpha}{\theta} = \left(\frac{U_L}{U_F + U_L} \right) = \frac{r}{1 + r}, \quad \text{where } r = \frac{U_L}{U_F}. \tag{7}$$

Equating the pressure loss for the two fluid streams in a parallel flow circuit, the following equation is satisfied:

$$\frac{f_F F_{d,F} U_F^2}{D_{h,F}} = \frac{f_L F_{d,L} U_L^2}{D_{h,L}}. \tag{8}$$

Here, f, F_d, D_h are the friction factor, flow depth, and hydraulic diameter, respectively. To first order, the hydraulic diameter of the two flow paths can be approximated by the channel widths between fins (d_F) and that between louvers (d_L), as shown in Fig. 7(b), and the flow depth ratio as $F_{d,F}/F_{d,L} = \cos\theta$. Both friction factors can be assumed proportional to a negative power of Reynolds number, $f = c/Re^e$. Assuming that the constant c, and exponent e are equal for the two fluid streams, the

ratio $f_F/f_L = (U_L d_L / U_F d_F)^e$. Hence, from Eq. (8), $U_L/U_F = r = (d_L/d_F)^{(1+e)/(2-e)} \cos^{1/(2-e)}\theta$. Substituting in Eq. (7), an expression for flow efficiency follows as:

$$\eta \propto \frac{d^{(1+e)/(2-e)}}{\cos^{1/(e-2)}\theta + d^{(1+e)/(2-e)}}, \tag{9}$$

where $d = d_L/d_F = (\sin(\theta) - b)/(F_p - \sin(\theta) - b\cos(\theta))$ is the characteristic *flow efficiency length scale ratio*.

The above formulation reveals the relationship between the flow efficiency and fin pitch ratio, thickness ratio, and louver angle. As the ratio $d \to 0$, $\eta \to 0$; conversely as $d \to \infty$, $\eta \to 1$. In reality though, for typical louver geometries, $0 < d < 1$. Eq. (9) relates the trends in flow efficiency to geometrical parameters, and it can be shown from Eq. (9) that $\eta \propto d$, i.e, η is a monotonic function of d.

The individual effect of the three geometrical parameters, fin pitch ratio, thickness ratio and louver angle on flow efficiency can be studied by evaluating their

effect on the ratio d. The derivatives of function d with respect to the three variables are written as:

$$d'_F = \frac{-1}{(F - \sin(\theta) - b\cos(\theta))^2},$$

$$d'_\theta = \frac{F\cos(\theta) - b - b\cos(\theta) + b\sin^2(\theta)}{(F - \sin(\theta) - b\cos(\theta))^2},$$

$$d'_b = \frac{-F + \sin(\theta) + b\cos(\theta) + \sin^2(\theta) - b\sin(\theta)}{(F - \sin(\theta) - b\cos(\theta))^2}.$$

To verify the relevance and importance of ratio d, we compare predicted trends in flow efficiency with known results and also validate some unexpected trends predicted by d. It can be seen that d'_F is always less than zero, so that increasing fin pitch ratio always has a negative effect on flow efficiency. Increasing louver angle has a positive effect on flow efficiency almost in all parameter ranges, except under some very unusual conditions, such as fin pitch ratio less than 1.0, louver angle larger than 70° and thickness ratio larger than 0.4 to satisfy the inequality $F\cos(\theta) - b - b\cos(\theta) + b^2\sin(\theta) < 0$. Increasing thickness ratio has a negative

effect on flow efficiency for large fin pitch ratios, and small louver angle. Conversely, for small fin pitch ratio (less than 1.0), and large louver angles (larger than 40°), increasing thickness, increases the flow efficiency.

Fig. 8(a) shows iso-surfaces of d at $d = 0.32$, 0.74 and 1.55. Generally, high values of d (and flow efficiency) are located in regions of large louver angles and small fin pitch ratios. Conversely, low values of d exist in regions of small louver angles and large fin pitches. Hence, the trends in d indicate that large louver angles can compensate for the loss in flow efficiency brought about by large fin pitches.

Fig. 8(b) shows contours of d at three louver angles, 10°, 30° and 40°. At a louver angle of 10°, ratio d is very small. Both fin pitch and thickness ratios have a very slight effect on d, and d decreases slightly as fin pitch and thickness ratio increase. At a louver angle of 30°, the effect of fin pitch and thickness ratio becomes more apparent. As louver angle increases to 40°, fin pitch has a significant effect on d. We note that the thickness ratio has two completely opposite effects at small and larger fin pitch ratios. For fin pitch ratios less than 1.1, d (flow efficiency) increases with increase of thickness ratio; at
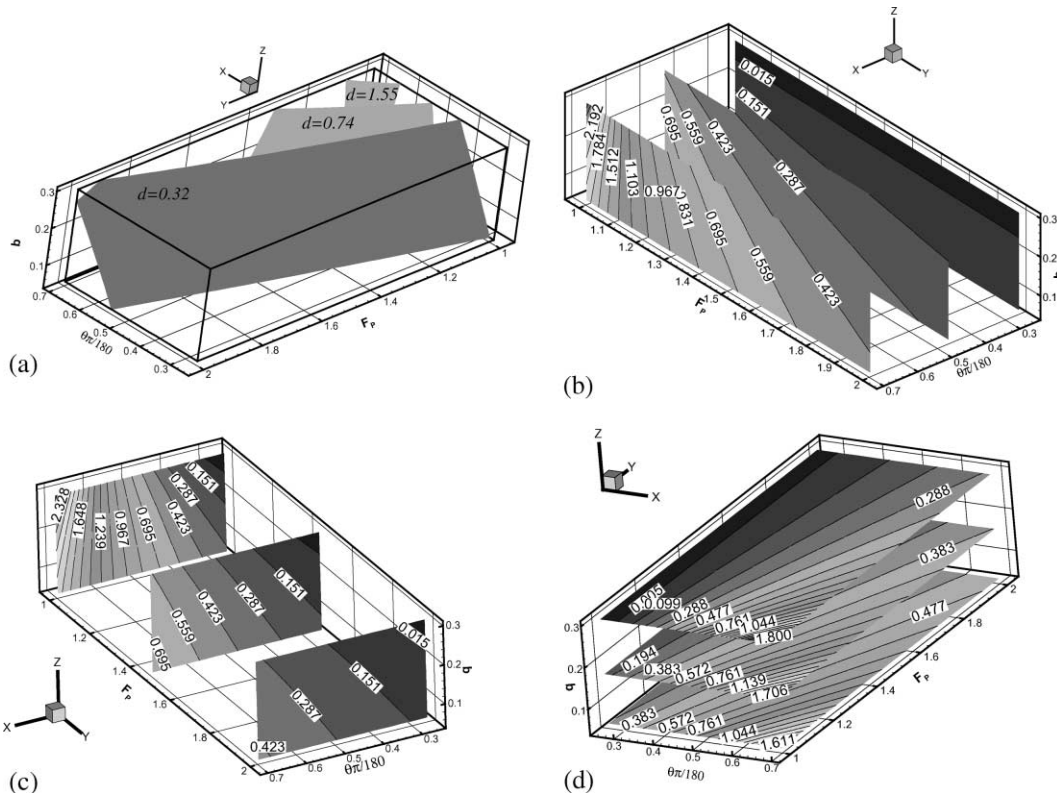

Fig. 8. Predicted trends from model. High values of d indicate high flow efficiency: (a) combined effect of three parameters on flow efficiency at three levels, $d = 0.32$, 0.74 and 1.55; (b) effect of fin pitch ratio and thickness ratio at three louver angles; (c) effect of louver angle and thickness ratio at three fin pitch ratios; (d) effect of fin pitch ratio and louver angle at three thickness ratios.

$F_p = 1.1$, d is not affected by thickness ratio; and for $F_p > 1.1$, d decreases with an increase in thickness ratio.

Fig. 8(c) plots the effect of louver angle and thickness ratio on d for three fin pitch ratios, 1.0, 1.5 and 2.0. It is found that louver angle has a strong effect on d at small fin pitch ratios, whereas the sensitivity of d to louver angle decreases as fin pitch increases. However, larger louver angles do compensate for high fin pitches by increasing d. We again note the trend reversal of the effect of thickness on d at large louver angles and small fin pitches. The normal trend, which is present for moderate to high fin pitches, and moderate to low louver angles, is a decrease in d and flow efficiency with an increase in thickness. The trend reversal can be seen clearly in Fig. 8(b) and (c) at $F_p = 1.0$, when the slope of constant d-lines change at around 40° louver angle. Although, counter-intuitive, the result is reasonable because for large louver angles, the percentage reduction of the fin gap caused by an increase in thickness ratio is smaller than the corresponding reduction of the gap between two louvers. This leads to conditions more favorable to louver directed flow. However large louver angles and thick louvers are prone to develop large recirculation zones on louvers at relatively low Reynolds numbers, which lowers the effective d, and subsequently the flow efficiency.

Finally, Fig. 8(d) plots the effect of louver angle and fin pitch ratio on d on planes of constant thickness. Consistent with previous results, flow efficiency (proportional to d) is higher for larger louver angles and smaller fin pitch ratios. The effect of fin pitch ratio and louver angle is more significant at larger fin thickness.
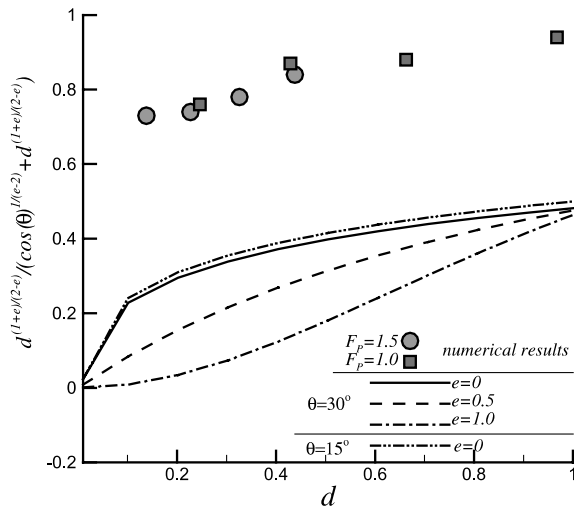
4.4. General correlation for flow efficiency

In the previous section, a first-order relationship between flow efficiency and geometrical parameters was introduced in Eq. (9). In this section, Eq. (9) is used as the foundation for developing a general correlation for flow efficiency. We first use Eq. (9) to set the value of flow efficiency based solely on trends predicted by geometrical information (given by η_1). This establishes the correct base trends in flow efficiency, and further corrections are added to match the absolute values. In the next step, an additive factor (given by η_2) is introduced to match the asymptotic value of flow efficiency for a given geometry. Finally, η_3 adjusts the asymptotic value
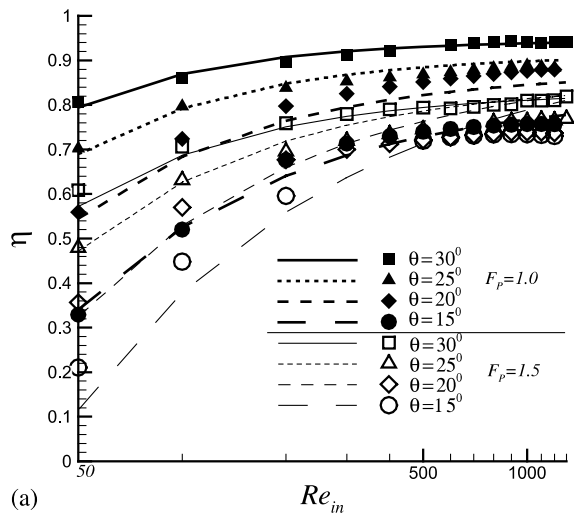
(a)
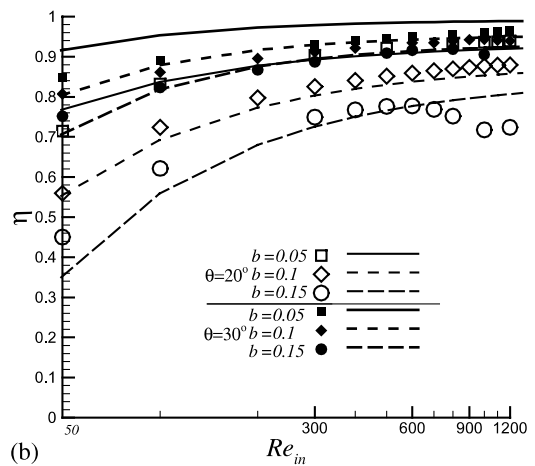
(b)

Fig. 10. Comparison of flow efficiencies obtained by Eq. (10) and numerical results. (a) Geometries with different louver angles and fin pitch ratios at a thickness ratio of 0.1; (b) geometries with different thickness ratio at fin pitch 1.0 and louver angles 20° and 30°.

Fig. 9. Comparison of the trends in asymptotic flow efficiency from numerical simulations with predicted model trends for different values of d. The exponent, $e = 0$ shows the best agreement.

by introducing a Reynolds number dependency. All, η_{1-3} are functions of the louver geometry, whereas, only η_3 has a Reynolds number dependence in it.

To obtain a reasonable value of the exponent e in Eq. (9), predicted trends with different values of e are compared to trends in asymptotic values of flow efficiency for different geometries (or different values of d). These are plotted in Fig. 9. It is found that $e \to 0$ gives the best representation of the trends seen in the asymptotic flow efficiencies. It is worth noting, that the exponent $e \to 0$, represents the limiting case for fully rough channels in which there is no or very little Reynolds number dependence of friction factor. Hence, the final form of the correlation is given by:

$$\eta = \eta_1 + \eta_2 + \eta_3, \tag{10}$$

where

$$\eta_1 = \frac{d^{1/2}}{d^{1/2} + 1/\cos^{1/2}(\theta)},$$

$$\eta_2 = \frac{0.357}{(F_p b)^{0.1}} \left(\frac{30}{\theta} \right)^{(F_p - 0.9)}$$

and

$$\eta_3 = -\frac{70b}{Re_{in}^{(0.38/F_p^{1.1} + 0.02\theta)}},$$

where

$$d = \frac{d_L}{d_F} = \frac{\sin(\theta) - b}{F_p - \sin(\theta) - b\cos(\theta)},$$

in the range $0.794 < F_p < 2.0$; $15° < \theta < 50°$; $0.05 < b < 0.2$; $50 < Re_{in} < 1200$; $0.1 < d < 1.9$.
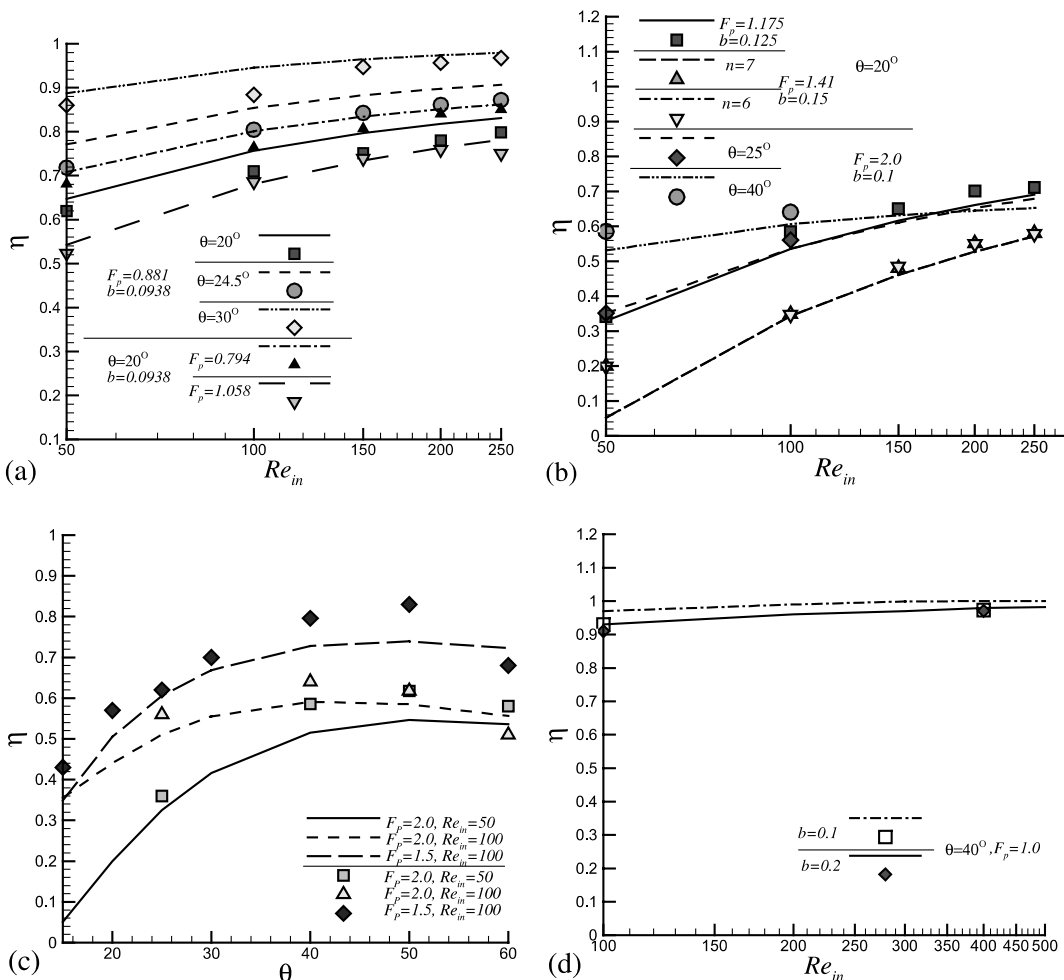

Fig. 11. Comparison of flow efficiency obtained from Eq. (10) with numerical calculations over a large range of fin pitch ratio (from 0.794 to 2.0) at different louver angles (from 20° to 60°) and thickness ratios (0.1 to 0.2). These data points were not used to construct the correlation.

Fig. 10 shows the comparison of flow efficiencies obtained from the above correlation and numerical calculations on which the correlation is based (cases in Table 1). The errors in the correlation are larger at low Reynolds numbers, small louver angles, and large fin pitches.

We further test the accuracy of the correlation by using it to predict flow efficiencies in louver configurations not used to construct the correlation. This is shown in Fig. 11. In these cases, fin pitch ratios vary from 0.794 to 2.0, louver angle from 20° to 40°, with different thickness ratios. The number of louvers, geometry of inlet, exit, and redirection louvers are also different from the geometries used to construct the correlation. The correlation predicts the flow efficiency with good accuracy. Additional comparisons are presented for extreme conditions of high louver angles and thick louvers. One set is for louvered fins with large louver angles (40°, 50°

and 60°) at two fin pitch ratios, 1.5 and 2.0, with a thickness ratio of 0.1, the other is for fins with two thickness ratios (0.1 and 0.2) at a large louver angle (40°) and a fin pitch ratio of 1.0. The complete geometrical parameters are described in Table 2. Fig. 11(c) and (d) plots the predicted flow efficiency versus the numerical calculations. Even for the extreme louver geometries, the correlation shows a high degree of accuracy in predicting the numerical data, up to $\theta = 50°$. The correlation does not predict the drop in flow efficiency for $\theta > 50°$, which is a result of blockages between louver passages caused by massive flow separation. Fig. 11(d) tests the prediction capability of the correlation at large thickness ratios. For small fin pitch, and high louver angle, the ratio d predicts an increasing trend in flow efficiency

Table 2
Summary of calculations at low Reynolds numbers with large louver angles and thickness ratios

F_p	b	θ	Re	F_d
1.5	0.1	25	50	13
		30		
		40		
		50		
		60		
2.0		25	50, 100	
		40		
		50		
		60		
1.0	0.1	40	100	
	0.2		400	
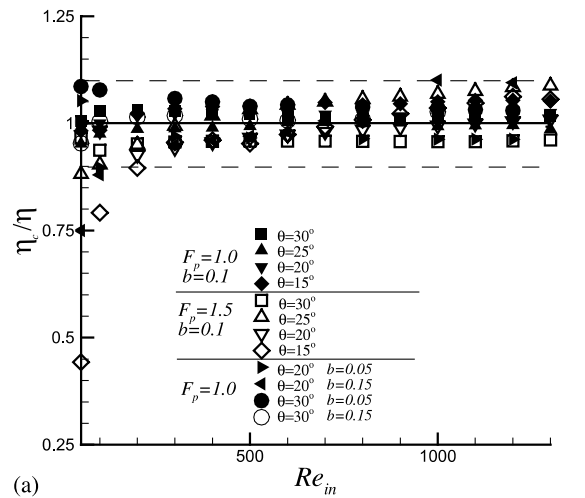
(a)
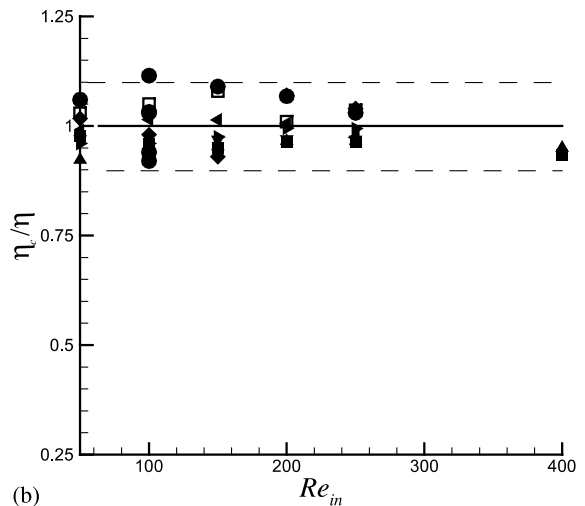
(b)

Fig. 13. Ratio of flow efficiency predicted by Eq. (10) to calculated flow efficiencies. Error within ±10% is bounded by dashed lines; (a) for the basic cases on which the correlation was based; (b) for all the other cases.

Fig. 12. Comparison of flow efficiency predicted by Eq. (10) and previous correlations.

with thickness. This is countered by recirculation zones which are more prevalent for thick louvers. Both these effects combine to give a near constant flow efficiency.

A comparison between the current and previous correlations is plotted in Fig. 12, for $F_p = 1.0$ and 1.5, louver angle 30°, and thickness ratio of 0.1. For $F_p = 1.0$, current results agree well with AC, whereas large differences are observed at $F_p = 1.5$ because of the fully developed assumptions. B's correlation gave the lowest values for both fin pitch ratios. The trends exhibited by SW's correlation are opposite to the other correlations.

Finally, Fig. 13(a) and (b) plots the prediction error of the current correlation. Results show that more than 95% of the calculation results are represented by the correlation within 10% error, with 80% of calculation results represented within 5%. The larger error at the Reynolds number of 100 in Fig. 13(b) is caused by the inclusion of the cases with large louver angles (50° and 60°).

5. Conclusions

Flow efficiency has a strong effect on the heat transfer capacity in multi-louvered fins. A review of past correlations has shown considerable differences in their ability to predict flow efficiency consistently and accurately. The present paper presents a general correlation for flow efficiency with the aid of a large database of high fidelity numerical simulations. Results show that flow efficiency is strongly dependent on geometrical parameters, especially at low Reynolds numbers. Flow efficiency increases with Reynolds number and louver angle, while decreasing with fin pitch and thickness ratio. Compared to fin pitch, louver angle has a stronger effect. Louver thickness effect on flow efficiency is also significant for small louver angles. A relationship for the trend in flow efficiency is developed based on geometrical and first-order hydrodynamic effects. The relationship is then supplemented by numerical results to develop a general correlation for flow efficiency with a geometrical dependence on fin pitch, louver thickness ratio, and louver angle. Comparisons show that the correlation represents more than 95% of numerical predictions within a 10% error band, and 80% of predictions within a 5% error band over a wide range of geometrical and hydrodynamic conditions.

References

[1] F.N. Beauvais, An Aerodynamic Look at Automobile radiators, SAE paper no. 650470, 1965.

[2] C.J. Davenport, Heat Transfer and Fluid Flow in Louvered Triangular Ducts, Ph.D. Thesis, CNAA, Lanchester Polytechnic, 1980.

[3] R.L. Webb, P. Trauger, Flow structure in the louvered fin heat exchanger geometry, Exp. Therm. Fluid Sci. 4 (1991) 205–217.

[4] A. Sahnoun, R.L. Webb, Prediction of heat transfer and friction for the louver fin geometry, J. Heat Transfer 114 (1992) 893–900.

[5] K.D. Bellows, Flow Visualization of Louvered-Fin Heat Exchangers, Masters Thesis, University of Illinois at Urbana-Champaign, 1996.

[6] N.C. DeJong, A.M. Jacobi, Flow, Heat Transfer, and Pressure Drop Interactions in Louvered-Fin Arrays, ACRC TR-146, University of Illinois at Urbana-Champaign, January 1999.

[7] A. Achaichia, T.A. Cowell, Heat transfer and pressure drop characteristics of flat tube and louvered plate fin surfaces, Exp. Therm. Fluid Sci. 1 (1988) 147–157.

[8] D.K. Tafti, L.W. Zhang, G. Wang, Time-dependent calculation procedure for fully developed and developing flow and heat transfer in louvered fin geometries, Numer. Heat Transfer, Part A 35 (1999) 225–249.